*Nanochem Res 4(1): 55-63, Winter and Spring 2019*

RESEARCH PAPER

# Nano-$Fe_3O_4$ attached to Crosslinked sulfonated polyacrylamide (Cross-PAA-$SO_3H$) as high performance catalyst for the synthesis of thiazoles under ultrasonic irradiations

***Hossein Shahbazi-Alavi [1,*] Javad Safaei-Ghomi [2]***

[1] *Young Researchers and Elite Club, Kashan Branch, Islamic Azad University, Kashan, Iran*

[2] *Department of Organic Chemistry, Faculty of Chemistry, University of Kashan, Kashan, Iran*

**ARTICLE INFO**

***Article History:***
*Received 21 January 2019*
*Accepted 08 May 2019*
*Published 15 June 2019*

***Keywords:***
*Thiazole*
*Nanocatalyst*
*Ultrasonic Irradiation*
*Polyacrylamide*
*Crosslink*

**ABSTRACT**

Nano-$Fe_3O_4$ attached to Cross-linked sulfonated polyacrylamide (Cross-PAA-$SO_3H$), as a superior catalyst, has been utilized for the preparation of 3-alkyl-4-phenyl-1,3-thiazole-2(3*H*)-thione derivatives through a three-component reaction of phenacyl bromide or 4-methoxyphenacyl bromide, carbon disulfide, and primary amine. The best results were gained in ethanol, and it was also found that the reaction gives convincing results in the presence of cross-PAA-$SO_3H$@nano-$Fe_3O_4$ (5 mg) under ultrasonic irradiation. The structures of the products were fully established on the basis of their $^1H$ NMR, $^{13}C$ NMR and FT-IR spectra. A proper, atom-economical, straightforward one-pot multicomponent synthetic route for the synthesis of 1,3-thiazoles in good yields has been devised using cross-linked sulfonated polyacrylamide (Cross-PAA-$SO_3H$) attached to nano-$Fe_3O_4$. The remarkable advantages of this methodology are short reaction times, high to excellent yields, operational simplicity, low catalyst loading and reusability of the catalyst. The catalyst has been characterized by Fourier-transform infrared spectroscopy (FT-IR), scanning electron microscope (SEM), X-ray powder diffraction (XRD), energy dispersive spectroscopy (EDS), thermo- gravimetric analysis (TGA) and vibrating-sample magnetometer (VSM).

**How to cite this article**
*Shahbazi-Alavi H, Safaei-Ghomi J. Nano-$Fe_3O_4$ attached to Crosslinked sulfonated polyacrylamide (Cross-PAA-$SO_3H$) as high performance catalyst for the synthesis of thiazoles under ultrasonic irradiations. Nanochem Res, 2019; 4(1):55-63. DOI: 10.22036/ncr.2019.01.007*

## INTRODUCTION

1,3-thiazoles possess many biological properties such as anticancer [1], antimicrobial [2], anti-inflammatory [3], and anti-candida [4]. Finding effective methods for the preparation of 1,3-thiazoles is a principal challenge. The synthesis of 1,3-thiazole derivatives have been reported in the presence of different catalysts including DBU [5], $HClO_4$-$SiO_2$ [6], $Bi(SCH_2COOH)_3$ [7], $[Et_3NH][HSO_4]$ [8], and Ytterbium(III) Triflate [9]. However, some of the reported methods endure drawbacks including long reaction times, harsh reaction conditions, use of toxic and non-reusable catalyst. To avoid the existing limitations, the exploration of an efficient catalyst with high catalytic activity and short reaction times for the preparation of 1,3-thiazoles is still favored. The feasibility of achieving one-pot multi-component synthesis under ultrasonic irradiation with a heterogeneous catalyst could improve the reactions rates and shorten the reactions times. The modifying cross-linked polyacrylamides make them attractive objects in chemistry and polymer science [10-12]. Sulfonated polyacrylamides have unique characteristics such as high strength, hydrophilicity, and proton conductivity [13-

* Corresponding Author Email: *hossien_shahbazi@yahoo.com*

14]. Recently, magnetic nanoparticles (MNPs) have been successfully utilized to immobilize enzymes, polymers, transition metal catalysts and organocatalysts [15-16]. The ultrasound approach decreases time, and increases yields of products by creating the activation energy in micro surroundings [17-18]. In the current study, we investigate an easy and rapid method for the synthesis of thiazole-2(3*H*)-thione through three-component reactions of phenacyl bromide or 4-methoxyphenacyl bromide, carbon disulfide and primary amine using cross-linked sulfonated polyacrylamide (Cross-PAA-$SO_3H$) attached to nano-$Fe_3O_4$, as an efficient catalyst under ultrasonic irradiations (Scheme 1).

## EXPERIMENTAL SECTION

*Chemicals and apparatus*

NMR spectra were obtained on a Bruker spectrometer with $CDCl_3$ as the solvent and TMS as an internal standard. Chemical shifts (δ) are given in ppm and coupling constants (J) are given in Hz. FT-IR spectra were recorded with KBr pellets by a Magna-IR, spectrometer 550 Nicolet. CHN compositions were measured by Carlo ERBA Model EA 1108 analyzer. Powder X-ray diffraction (XRD) was performed on a Philips diffractometer of X'pert Company with monochromatized Cu Kα radiation (λ = 1.5406 Å). Microscopic morphology of products was visualized by SEM (MIRA3). The thermogravimetric analysis (TGA) curves are registered using a V5.1A DUPONT 2000. The magnetic measurement of samples was performed in a vibrating sample magnetometer (VSM) (Meghnatis Daghigh Kavir Co.; Kashan Kavir; Iran).

*Preparation of Cross-linked Sulfonated Polyacrylamide (Cross-PAA-$SO_3H$):*

In a round-bottom flask (200 mL) equipped with magnetic stirrer and condenser, 5 gr of acrylamid (AAM) (70 mmol) and 5.17 gr of 2-acryloylamino-2-methylpropane-sulfonic acid (25 mmol) (AAMPS), (approximately AAM/AAMPS (3/1)) and 0.77 gr of N,N-methylene-bis-acrylamid (NNMBA) (5 mmol), as a crosslinking agent and benzoyl peroxide, as an initiator, were added to 80 mL EtOH under reflux condition for 5 h. After completion of reaction, the white precipitate was formed, filtered, washed and dried in a vacuum oven at 70°C for 12 h. The weight of polymer was 10.1 gr with the yield of 91.8%. This catalyst was characterized with infrared spectroscopy and back titration acid-base to confirm sulfonation and determine accurate sulfonation levels. Acidic capacity of this catalyst was estimated to be 1.1 mmol /gr.

*Preparation of cross-linked solfonated polyacrylamide@nano-$Fe_3O_4$*

1 gr of synthesized polymers was poured in 100 mL round bottom flask under stirring at room-temperature, then 50 mL HCl (0.4 M) was added to it. Our target molecules was synthesized by magnetic nanocatalyst with mass ratio polymer/nano-$Fe_3O_4$ = 2/1. So, 0.43 gr (2.1 mol) $FeCl_2.4H_2O$ and 1.17 gr (2×2.1) $FeCl_3.6\ H_2O$ were added and the mixture was stirred until dissolved completely (flask1). In another 500 ml round-bottom flask, No 2, 400 mL aqueous solution of $NH_3$ (0.7M) was poured under argon gas. Then, flask 1 was added to flask 2 immediately. Nanocatalyst was filtered and washed with water (2×25 mL) and dried in an oven at 50 ° C.

*General procedure for the synthesis of 1,3-thiazoles*

A mixture of primary amine (1.0 mmol) and carbon disulfide (1.0 mmol) in ethanol (8 mL) was stirred for 5 min, and then phenacyl bromide or 4-methoxyphenacyl bromide (1.0 mmol) and Cross-PAA-$SO_3H$ attached to nano-$Fe_3O_4$ (5 mg) were added and sonicated at 40 W power for the appropriate times (monitored by TLC). After completion of the reaction, the nanocatalyst was easily separated using an external magnet. The solvent was evaporated and the solid obtained

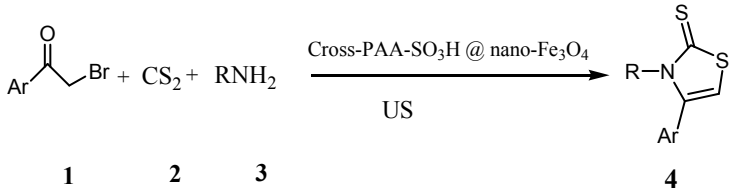


**1** **2** **3** **4**

Scheme 1. Synthesis of 1,3-thiazoles under ultrasonic irradiation

was washed with EtOH to get pure product. The characterization data of the compounds are given below.

*3-Benzyl-4-phenyl-1,3-thiazole-2(3H)-thione* (**4a**): Colorless viscous oil; FT-IR (KBr): $\overline{\nu}$ = 3102, 3005, 1602, 1479, 1202 $cm^{-1}$; $^1H$ NMR (250 MHz, $CDCl_3$): $\delta$ 4.90 (s, 2H, $CH_2$), 6.03 (s, 1H, CH of alkene), 6.95–7.36 (m, 10H, CH, ArH). $^{13}C$ NMR (62.5 MHz, $CDCl_3$): $\delta$ 47.24, 98.85, 127.06, 127.42, 128.52, 128.55, 129.08, 133.32, 137.45, 154.85, 178.37, 197.18. MS (EI, 70 eV): *m*/*z* (%) = 283 (5), 267(68), 181(7), 91 (100), 77 (4), 65 (12), 45 (4). Anal. Calcd. for $C_{16}H_{13}NS_2$ (283): C, 67.81; H, 4.62; N, 4.94. Found: C, 67.70; H, 4.52; N, 4.73 %.

*3-(3,4-dichlorobenzyl)-4-phenyl-1,3-thiazole-2(3H)-thione* (**4b**): Colorless viscous oil; FT-IR (KBr): $\overline{\nu}$ = 3152, 3004, 1628, 1603, 1477, 1302, 1104 $cm^{-1}$. $^1H$ NMR (250 MHz, $CDCl_3$): $\delta$ 4.83 (s, 2H, $CH_2$), 6.05 (CH of alkene), 6.75–7.97 (m, 8H, CH of ArH). $^{13}C$ NMR (62.5 MHz, $CDCl_3$): $\delta$ 46.07, 99.25, 126.72, 128.65, 128.74, 129.35, 129.66, 133.54, 130.50, 135.38, 136.62, 137.21, 172.70, 194.15. Anal. Calcd. for $C_{16}H_{11}Cl_2NS_2$ (350): C, 54.55; H, 3.15; N, 3.98. Found: C, 54.36; H, 3.05; N, 3.84 %.

*3 - ( 2- Naphthyl methyl ) - 4 - phenyl - 1, 3 - thiazole 2(3H)- thione* (**4c**): Colorless viscous oil; FT-IR (KBr): $\overline{\nu}$ = 3102, 3009, 1652, 1605, 1479, 1204 $cm^{-1}$. $^1H$ NMR (250 MHz, $CDCl_3$): $\delta$ 3.95 (s, 2H, $CH_2$), 6.12 (s, 1H, CH of alkene), 6.92–7.97 (m, 12H, CH of ArH). $^{13}C$ NMR (62.5 MHz, $CDCl_3$): $\delta$ 45.35, 99.05, 123.77, 125.32, 125.84, 126.34, 128.06, 128.68, 128.75, 133.54, 122.52, 129.28, 131.50, 135.08, 172.44, 194.16. Anal. Calcd. for $C_{20}H_{15}NS_2$ (333): C, 72.03; H, 4.53; N, 4.20. Found: C, 72.05; H, 4.40; N, 4.15 %.

*3-(2-Furyl methyl)-4-phenyl-1,3-thiazole-2(3H)-thione* (**4d**): Colorless viscous oil; FT-IR (KBr): $\overline{\nu}$ = 3105, 3002, 1653, 1607, 1474, 1202 $cm^{-1}$. $^1H$ NMR (250 MHz, $CDCl_3$): $\delta$ 4.84 (s, 2H, $CH_2$), 6.10 (s, 1H, CH of alkene), 6.22 (1H, CH of furan), 7.25–8.05 (m, 7H, CH of ArH and CH of furan). $^{13}C$ NMR (62.5 MHz, $CDCl_3$): $\delta$ 44.25, 98.32, 109.52, 110.83, 127.08, 128.76, 129.58, 142.12, 144.54, 147.92, 155.44, 192.18. Anal. Calcd. for $C_{14}H_{11}NOS_2$ (273): C, 61.51; H, 4.06; N, 5.12. Found: C, 61.46; H, 4.04; N, 5.09 %.

*3-(4-Fluorobenzyl)-4-phenyl-1,3-thiazole-2(3H)-thione* (**4e**): Colorless viscous oil; FT-IR (KBr): $\overline{\nu}$ = 3153, 3005, 1628, 1604, 1473, 1302, 1108 $cm^{-1}$. $^1H$ NMR (250 MHz, $CDCl_3$): $\delta$ 4.85 (s, 2H, CH2), 6.05 (s, 1H, CH of alkene), 6.85 (d, 2H, *J* = 6.8 Hz, CH arom), 7.02–7.59 (m, 5H, CH of ArH), 7.98 (d, 2H, *J* = 7.5 Hz, CH of ArH).$^{13}C$ NMR (62.5 MHz, $CDCl_3$): $\delta$ 46.45, 99.08, 114.53, 128.67, 128.78, 133.51, 129.05, 135.46, 137.57, 153.28, 159.50, 194.19. Anal. Calcd. for $C_{16}H_{12}FNS_2$ (301): C, 63.76; H, 4.01; N, 4.65. Found: C, 63.60; H, 4.04; N, 4.42 %.

*3-(2-Methoxybenzyl)-4-phenyl-1,3-thiazole-2(3H) -thione* (**4f**): Colorless viscous oil; FT-IR (KBr): $\overline{\nu}$ = 3150, 3000, 1650, 1600, 1470, 1200, 1100 $cm^{-1}$. $^1H$ NMR (250 MHz, $CDCl_3$): $\delta$ 3.62 (s, 3H, $OCH_3$), 4.90 (s, 2H, $CH_2$), 6.03 (s, 1H, CH of alkene), 6.71–7.98 (m, 9H, CH, ArH).$^{13}C$ NMR (62.5 MHz, $CDCl_3$): $\delta$ 42.56, 55.05, 98.47, 110.05, 120.53, 128.38, 128.46, 128.55, 128.78, 129.05, 133.54, 127.12, 135.45, 156.35, 194.14. Anal. Calcd. for $C_{17}H_{15}NOS_2$ (313): C, 65.14; H, 4.82; N, 4.47. Found: C, 65.03; H, 4.74; N, 4.35%.

*3-(4-Methylbenzyl)-4-(4-methoxyphenyl)-1,3-thiazole-2(3H)-thione* (**4g**): Colorless viscous oil; FT-IR (KBr): $\overline{\nu}$ = 3156, 3008, 1648, 1612, 1475, 1206, 1108 $cm^{-1}$. $^1H$ NMR (250 MHz, $CDCl_3$): $\delta$ 2.23 (s, 3H, $CH_3$), 3.86 (s, 3H, $OCH_3$), 4.95 (s, 2H, CH2), 5.98 (s, 1H, CH of alkene), 6.82–7.35 (m, 8H, CH of ArH).$^{13}C$ NMR (62.5 MHz, $CDCl_3$): $\delta$ 21.35, 48.54, 55.95, 98.68, 115.38, 123.42, 125.64, 130.65, 131.25, 132.59, 139.25, 160.20, 174.25, 183.56. Anal. Calcd. for $C_{18}H_{17}NOS_2$ (327): C, 66.02; H, 5.23; N, 4.28;. Found: C, 65.90; H, 5.14; N, 4.12 %.

*3-benzyl-4-(4-methoxyphenyl)-1,3-thiazole-2 (3H)-thione* (**4h**): Colorless viscous oil; FT-IR (KBr): $\overline{\nu}$ = 3157, 3012, 1645, 1616, 1478, 1209, 1107 $cm^{-1}$. $^1H$ NMR (250 MHz, $CDCl_3$): $\delta$ 3.89 (s, 3H, $OCH_3$), 5.25 (s, 2H, $CH_2$), 6.28 (s, 1H, CH of alkene), 6.85–7.39 (m, 9H, CH of ArH).$^{13}C$ NMR (62.5 MHz, $CDCl_3$): $\delta$ 48.50, 55.37, 99.86, 110.55, 114.54, 122.54, 128.38, 129.54, 132.86, 137.54, 145.68, 160.85, 185.36. MS (EI, 70 eV): *m*/*z* (%) = 313 (M). Anal. Calcd. for $C_{17}H_{15}NOS_2$ (313): C, 65.14; H, 4.82; N, 4.47; Found: C, 65.02; H, 4.56; N, 4.34; %.

*3-(2-Furyl methyl)-4-(4-methoxyphenyl)-1,3-thiazole-2(3H)-thione* (**4i**): Colorless viscous oil; FT-IR (KBr): $\overline{\nu}$ = 3144, 3012, 1658, 1615, 1478, 1209, 1112 $cm^{-1}$. $^1H$ NMR (250 MHz, $CDCl_3$): $\delta$ 3.88 (s, 3H, $OCH_3$), 4.82 (s, 2H, CH2), 5.98 (2H, CH of furan), 6.20 (s, 1H, CH of alkene), 6.75–7.42 (m, 5H, CH of furan and CH of ArH). $^{13}C$ NMR (62.5 MHz, $CDCl_3$): $\delta$ 41.35, 55.34, 98.36, 108.35, 110.35, 118.35, 122.54, 130.22, 138.54, 142.35, 150.65, 161.25, 178.25. Anal. Calcd. for $C_{15}H_{13}NO_2S_2$ (303): C, 59.38; H, 4.32; N, 4.62; Found: C, 59.15; H, 4.14; N, 4.42%.

*3-(2-methoxybenzyl)-4-(4-methoxyphenyl)-1,3-thiazole-2(3H)-thione* (**4j**): Colorless viscous oil; FT-IR (KBr): $\overline{\nu}$ = 3142, 3010, 1654, 1611, 1472, 1205, 1116 $cm^{-1}$. $^1H$ NMR (250 MHz, $CDCl_3$): $\delta$ 3.68 (s, 3H, $OCH_3$), 3.84 (s, 3H, $OCH_3$), 4.89 (s, 2H, $CH_2$), 6.05 (s, 1H, CH of alkene), 6.72–7.53 (m, 8H, CH of ArH). $^{13}C$ NMR (62.5 MHz, $CDCl_3$): $\delta$ 43.54, 56.45, 56.48, 98.45, 110.25, 115.28, 120.54, 122.54, 125.85, 125.64, 128.54, 130.42, 138.20, 158.64, 160.24, 172.54. Anal. Calcd. for $C_{18}H_{17}NO_2S_2$ (343): C, 62.94; H, 4.99; N, 4.08; Found: C, 62.72; H, 4.70; N, 3.91. %.

## RESULTS AND DISCUSSION

*Characterization of the nanocatalyst*

In this study, we synthesized the cross-linked sulfonated polyacrylamide (Cross-PAA-$SO_3H$) with simultaneous radical co-polymerization in the presence of initiator and cross-linking agent. The FT-IR absorbance spectra of the dried cross-linked sulfonated polyacrylamide (poly AAM-*co*-AAMPS), $Fe_3O_4$ and Cross-PAA-$SO_3H$@nano-$Fe_3O_4$ are shown in Fig. 1. AAM is abbreviation of acrylamide, and AAMPS is abbreviation of 2-acrylamido-2-methylpropanesulfonic acid. The N–H stretching vibration of the amide groups in AAm and AAMPS and overlapping O–H stretching vibration of sulfonic acid group in AAMPS are observed in the region 3100–3500 $cm^{-1}$. The strong absorption band in the 1658 $cm^{-1}$ can be attributed to the stretching vibrations of C=O groups in both AAm and AAMPS. Secondary amide band of AAMPS unit has a peak in 1545 $cm^{-1}$. The sharp peak at 1042 $cm^{-1}$ is related to sulfonic acid (–$SO_3H$) group. The symmetric band of $SO_2$ is observed in 1178-1216 $cm^{-1}$. The band at 1453 $cm^{-1}$ is assigned to the stretching vibration of the C–N bond (amide) and the asymmetric bending of the C–H bond in methyl groups of AMPS. Table 1 gives the main characteristic peak assignment of the FT-IR spectra. Also a schematic illustration of the reaction is shown in Scheme 2. The absence of the olefinic band at 1620–1635 $cm^{-1}$ confirms that there

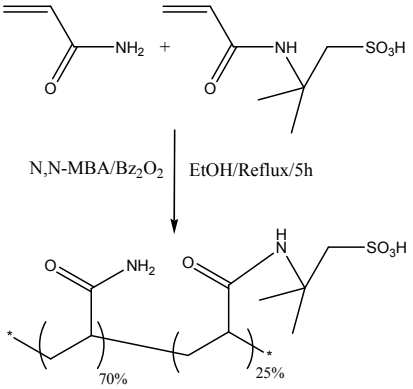


5% Crosslinked Sulfonated Polyacrylamide

Scheme 2. Preparation of cross-linked sulfonated polyacrylamide (Cross-PAA-$SO_3H$)

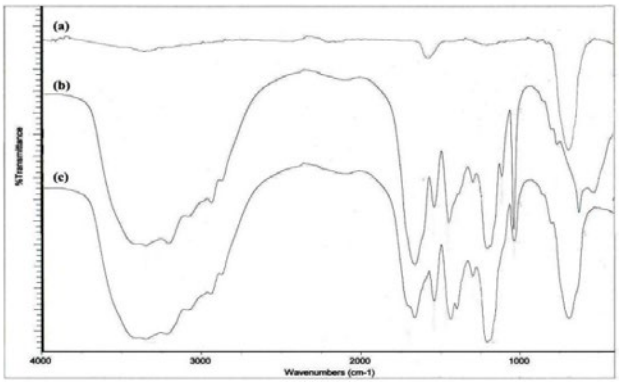


Fig. 1. The FT-IR spectra of (a) $Fe_3O_4$ NPs, (b) Cross-PAA-$SO_3H$, and (c) Cross-PAA-$SO_3H$@nano-$Fe_3O_4$

Table 1. Peak assignment of cross-linked sulfonated polyacrylamide (Cross-PAA-$SO_3H$)

| Peak position ($cm^{-1}$) | Assignment |
|---|---|
| 3100-3500 | N-H stretching of $NH_2$,OH stretching of (- $SO_3H$) |
| 1658 | C=O stretching of CO in AAM and AAMPS |
| 1545 | Secondary amid band of AAMPS |
| 1042 | Sulfonic acid (- $SO_3H$) group |
| 1175-1216 | Symmetric band of $SO_2$ |
| 1453 | Stretching of the C-N band (amid) |

is no residual monomer in the system. The results in Fig. 1 (c) suggest the integration of $Fe_3O_4$ NPs and Cross-PAA-$SO_3H$.

The particle size and morphology of Cross-PAA-$SO_3H$@nano-$Fe_3O_4$ were determined by Scanning Electronic Microscopy (SEM). The statistic of results from SEM images clearly demonstrates that the average size of Cross-PAA-$SO_3H$@nano-$Fe_3O_4$ is about 7-25 nanometers (Fig. 2).

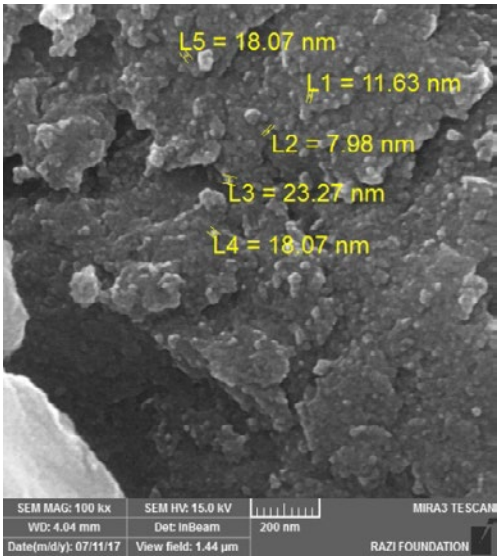


Fig. 2. SEM image of Cross-PAA-$SO_3H$@nano-$Fe_3O_4$

Fig. 3 exhibits the powder X-ray diffraction (XRD) pattern. The pattern agrees well with the reported pattern for $Fe_3O_4$ (JCPDS No. 75-1609). The particle size diameter (D) of the nanoparticles has been calculated by the Debye–Scherrer equation ($D = K\lambda/\beta \cos\theta$), where β FWHM (full-width at half-maximum or half-width) is in radian and θ is the position of the maximum of the diffraction peak. K is the so-called shape factor, which usually takes a value of about 0.9, and λ is the X-ray wavelength (1.5406Å for CuKα). All the strong peaks appeared at 2θ = 30.08°, 35.40°, 43.17°, 53.59°, 57.20°, 62.86°, and 74.02° can be easily indexed to nano-$Fe_3O_4$. The crystallite size of Cross-PAA-$SO_3H$@nano-$Fe_3O_4$ calculated by the Debye–Scherer equation is about 20-25 nm, in good agreement with the result obtained by SEM.

An EDS (energy dispersive X-ray) spectrum of Cross-PAA-$SO_3H$@nano-$Fe_3O_4$ (Fig. 4) exhibits

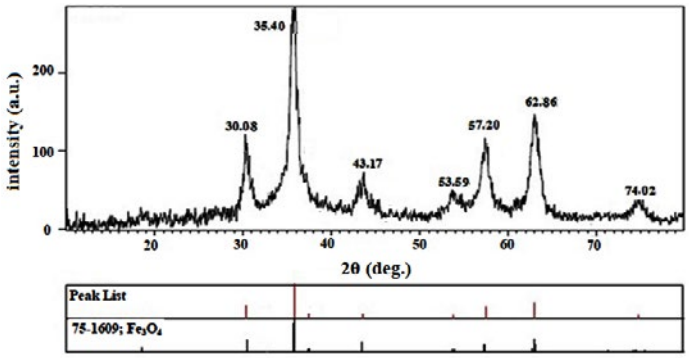


Fig. 3. The XRD pattern of Cross-PAA-$SO_3H$@nano-$Fe_3O_4$

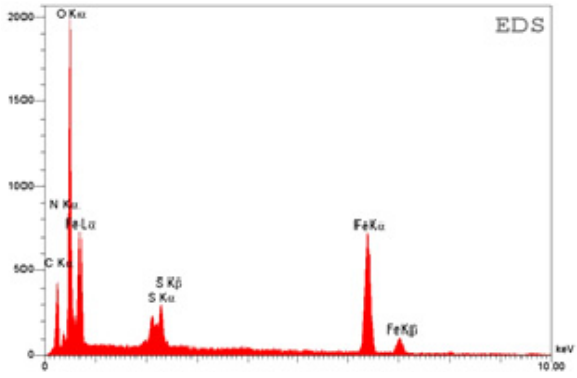


Fig. 4. EDS spectrum of Cross-PAA-$SO_3H$@nano-$Fe_3O_4$.

that the elemental compositions are carbon, oxygen, sulfur, iron and nitrogen.

The magnetic attributes of nano-$Fe_3O_4$ and Cross-PAA-$SO_3H$@nano-$Fe_3O_4$ were given with the help of a vibrating sample magnetometer (VSM) (Fig. 5). The amounts of saturation-magnetization for nano-$Fe_3O_4$ and Cross-PAA-$SO_3H$@nano-$Fe_3O_4$ are 47.2 emu/g and 26.8 emu/g. These results illustrate that the magnetization property is reduced by coating and functionalization.

Thermogravimetric analysis (TGA) evaluates the thermal stability of the Cross-PAA-$SO_3H$@nano-$Fe_3O_4$. These nanoparticles display proper thermal stability without a significant decrease in weight (Fig. 6). The weight loss at temperatures below 200°C is owing to the removal of physically adsorbed solvent and surface hydroxyl groups. The curve shows a weight loss about 20% from 250 to 600°C, resulting from the decomposition of the organic spacer attaching to the nano-$Fe_3O_4$ surface.

Table 2. Optimization of reaction conditions [a]

| Entry | Solvent (reflux) | Catalyst | Time (min) | Yield (%)[b] |
|---|---|---|---|---|
| 1 | EtOH | — | 500 | 39 |
| 2 | EtOH | CAN (5 mol %) | 250 | 51 |
| 3 | EtOH | $NaHSO_4$ (4 mol %) | 300 | 40 |
| 4 | EtOH | $InCl_3$ (4 mol%) | 200 | 56 |
| 5 | EtOH | $ZrO_2$ (3 mol%) | 250 | 45 |
| 6 | EtOH | *p*-TSA (3 mol%) | 200 | 64 |
| 7 | EtOH | nano-$Fe_3O_4$ (10 mg) | 200 | 52 |
| 8 | $H_2O$ (US: 40 W)[c] | Cross-PAA-$SO_3H$@nano-$Fe_3O_4$ (5 mg) | 15 | 75 |
| 9 | DMF (US: 40 W) | Cross-PAA-$SO_3H$@nano-$Fe_3O_4$ (5 mg) | 15 | 80 |
| 10 | $CH_3CN$ (US: 40 W) | Cross-PAA-$SO_3H$@nano-$Fe_3O_4$ (5 mg) | 10 | 88 |
| 11 | EtOH (US: 40 W) | Cross-PAA-$SO_3H$@nano-$Fe_3O_4$ (3 mg) | 10 | 91 |
| 12 | EtOH (US: 40 W) | Cross-PAA-$SO_3H$@nano-$Fe_3O_4$ (5 mg) | 10 | 93 |
| 13 | EtOH (US: 40 W) | Cross-PAA-$SO_3H$@nano-$Fe_3O_4$ (7 mg) | 10 | 93 |

[a] Phenacyl bromide (1 mmol), carbon disulfide (1 mmol), and benzyl amine (1 mmol)
[b] Isolated yield
[c] Ultrasonic irradiation

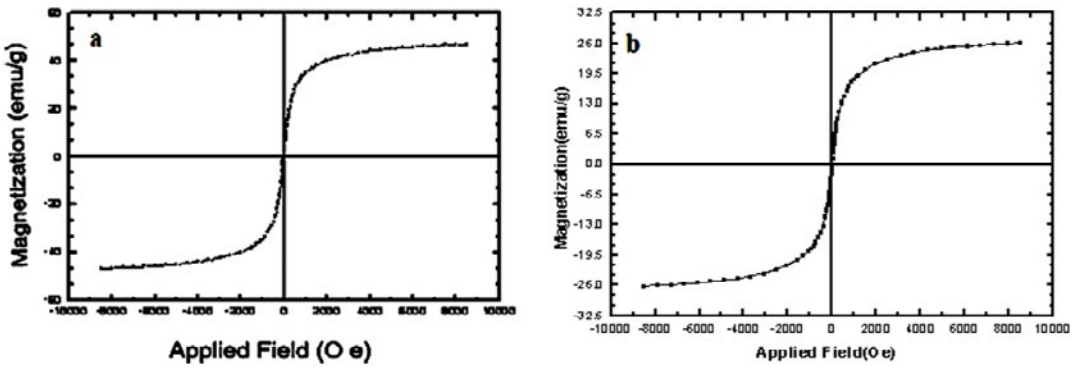


Fig. 5. The VSM curve of: (a) nano-$Fe_3O_4$ and (b) Cross-PAA-$SO_3H$@nano-$Fe_3O_4$

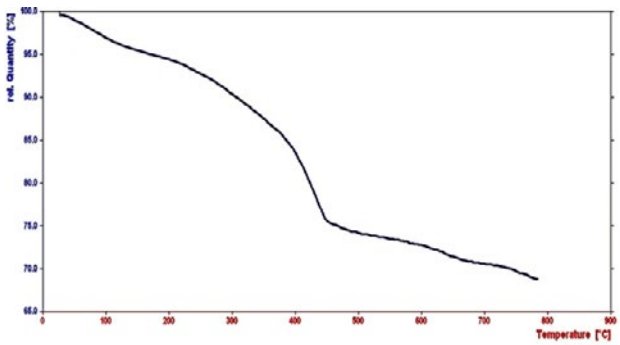


Fig. 6. TGA curve of Cross-PAA-$SO_3H$@nano-$Fe_3O_4$.

Table 3. Synthesis of thiazoles using Cross-PAA-$SO_3H$@nano-$Fe_3O_4$

| Entry | Amine (R-$NH_2$) | $ArCOCH_2Br$ | product | Time (min) | Yield (%)[a] |
|---|---|---|---|---|---|
| 1 | 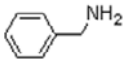 | 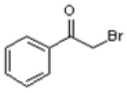 | **4a** | 10 | 93 |
| 2 | 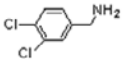 | 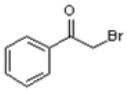 | **4b** | 10 | 85 |
| 3 | 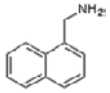 | 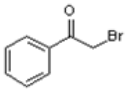 | **4c** | 15 | 84 |
| 4 | 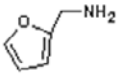 | 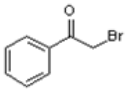 | **4d** | 15 | 90 |
| 5 | 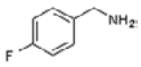 | 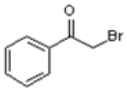 | **4e** | 10 | 88 |
| 6 | 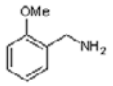 | 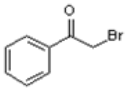 | **4f** | 10 | 92 |
| 7 | 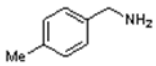 | 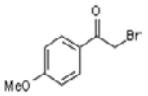 | **4g** | 15 | 87 |
| 8 | 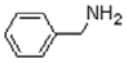 | 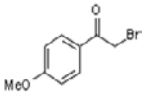 | **4h** | 10 | 82 |
| 9 | 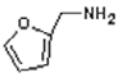 | 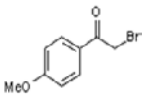 | **4i** | 10 | 80 |
| 10 | 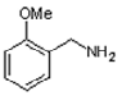 | 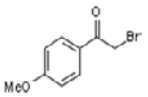 | **4j** | 10 | 86 |

[a] Isolated yield

*Catalytic behaviors of Cross-PAA-$SO_3H$@nano-$Fe_3O_4$ for the synthesis of 1,3-thiazoles*

Initially, the conditions for the synthesis of 3- alkyl -4 – phenyl -1,3 –thiazole -2(3*H*) -thione derivatives were optimized by the reaction of phenacyl bromide, carbon disulfide and benzyl amine as a model reaction. The model reactions were performed by CAN, $NaHSO_4$, $InCl_3$, $ZrO_2$, *p*-TSA, nano-$Fe_3O_4$ and Cross-PAA-$SO_3H$@nano-$Fe_3O_4$. The reactions were tested using various solvents including ethanol, acetonitrile, water, and dimethylformamide. The best results were

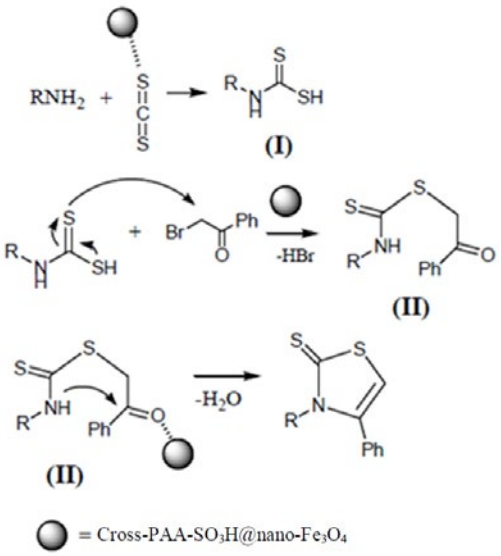


Scheme 3. Proposed reaction pathway for the synthesis of 1,3-thiazoles

gained in EtOH. The reaction gave convincing results in the presence of cross-PAA-$SO_3H$@nano-$Fe_3O_4$ (5 mg) under ultrasonic irradiation (Table 2). We studied the feasibility of the reaction by selecting some representative substrates (Table 2). To investigate the extent of this catalytic process, phenacyl bromide or 4-methoxyphenacyl bromide, carbon disulfide and primary amine were elected as substrates. Seeking of the reaction scope demonstrated that various primary amines can be utilized in this method (Table 3).

Scheme 3 displays a proposed mechanism for this reaction in the presence of cross-PAA-$SO_3H$@nano-$Fe_3O_4$ as the catalyst. Initially the nucleophilic attack by amines on a carbon disulfide generates intermediate (I). The next step involves nucleophilic attack of intermediate (I) on the methylene carbon of phenacyl bromide, leading to intermediate (II), and then ring closure by intramolecular attack of nitrogen at the carbonyl carbon to afford the 3-alkyl-4-phenyl-1,3- thiazole-2(3*H*)-thione derivatives. In this mechanism, the surface atoms of cross-PAA-$SO_3H$@nano-$Fe_3O_4$ activate the C=S and C=O groups for better reaction with nucleophiles.

The reusability of Cross-PAA-$SO_3H$@nano-$Fe_3O_4$ was studied for the reactions of phenacyl bromide, carbon disulfide and benzyl amine. It was found that the product yields are reduced to a small extent on each reuse (run 1, 93%; run 2, 93%; run 3, 92%; run 4, 92%; run 5, 91%; run 6, 90%;). After completion of the reaction, the nanocatalyst

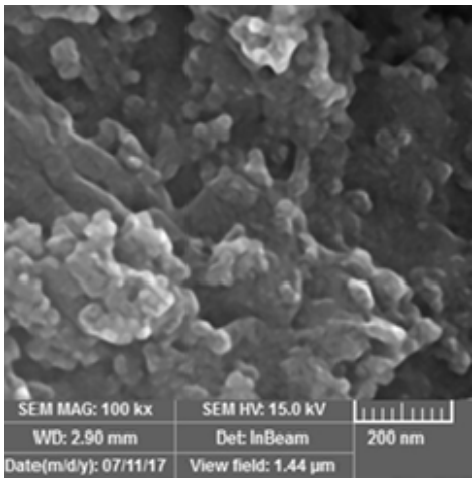


Fig. 7. SEM of Cross-PAA-$SO_3H$@nano-$Fe_3O_4$ after six times reuse

was separated by an external magnet. The catalyst was washed four times with ethanol and dried at room temperature for 18 h. The catalyst could be reused for six times with a minimal loss of activity. The morphology and particle size of Cross-PAA-$SO_3H$@nano-$Fe_3O_4$ were investigated by scanning electron microscopy (SEM) before use and after six times reuse with images shown in Fig. 7. The SEM of Cross-PAA-$SO_3H$@nano-$Fe_3O_4$ after reaction showed identical shape. The morphology of the nanoparticles remained unchanged before and after reaction. We believe that this is also the possible reason for the extreme stability of the nanoparticles presented herein.

## CONCLUSION

In conclusion, we have reported an efficient way for the synthesis of 3-alkyl-4-phenyl-1,3-thiazole-2(3*H*)-thione derivatives using cross-PAA-$SO_3H$@nano-$Fe_3O_4$ under ultrasonic irradiation. The method offers several advantages including easy availability, high yields, shorter reaction time, reusability of the catalyst, and low catalyst loading.

## CONFLICT OF INTEREST

The authors declare that there is no conflict of interests regarding the publication of this manuscript.

## REFERENCES

[1] Dawood KM, Gomha SM. Synthesis and Anti-cancer Activity of 1,3,4-Thiadiazole and 1,3-Thiazole Derivatives Having 1,3,4-Oxadiazole Moiety. Journal of Heterocyclic Chemistry. 2014;52(5):1400-5.

[2] Abdel-Wahab BF, Abdel-Aziz HA, Ahmed EM. Synthesis and antimicrobial evaluation of some 1,3-thiazole,

1,3,4-thiadiazole, 1,2,4-triazole, and 1,2,4-triazolo[3,4-b] [1,3,4]-thiadiazine derivatives including a 5-(benzofuran-2-yl)-1-phenylpyrazole moiety. Monatshefte für Chemie - Chemical Monthly. 2008;140(6):601-5.

[3] Sharma RN, Xavier FP, Vasu KK, Chaturvedi SC, Pancholi SS. Synthesis of 4-benzyl-1,3-thiazole derivatives as potential anti-inflammatory agents: An analogue-based drug design approach. Journal of Enzyme Inhibition and Medicinal Chemistry. 2009;24(3):890-7.

[4] Maillard LT, Bertout S, Quinonéro O, Akalin G, Turan-Zitouni G, Fulcrand P, et al. Synthesis and anti-Candida activity of novel 2-hydrazino-1,3-thiazole derivatives. Bioorganic & Medicinal Chemistry Letters. 2013;23(6):1803-7.

[5] Masquelin T, Obrecht D. A new general three component solution-phase synthesis of 2-amino-1,3-thiazole and 2,4-diamino-1,3-thiazole combinatorial libraries. Tetrahedron. 2001;57(1):153-6.

[6] Kumar D, Sonawane M, Pujala B, Jain VK, Bhagat S, Chakraborti AK. Supported protic acid-catalyzed synthesis of 2,3-disubstituted thiazolidin-4-ones: enhancement of the catalytic potential of protic acid by adsorption on solid supports. Green Chemistry. 2013;15(10):2872.

[7] Foroughifar N, Ebrahimi S. One-pot synthesis of 1,3-thiazolidin-4-one using Bi(SCH2COOH)3 as catalyst. Chinese Chemical Letters. 2013;24(5):389-91.

[8] Subhedar DD, Shaikh MH, Arkile MA, Yeware A, Sarkar D, Shingate BB. Facile synthesis of 1,3-thiazolidin-4-ones as antitubercular agents. Bioorganic & Medicinal Chemistry Letters. 2016;26(7):1704-8.

[9] Su W, Liu C, Shan W. Ytterbium(III) Triflate Catalyzed One-Pot Synthesis of 1,3-Thiazolidin-2-imines from Epichlorohydrin and Thioureas. Synlett. 2008;2008(05):725-7.

[10] Shach-Caplan M, Narkis M, Silverstein MS. Modification of porous suspension-PVC particles by stabilizer-free aqueous dispersion polymerization of absorbed monomers. Polymer Engineering & Science. 2002;42(5):911-24.

[11] Tamami B, Ghasemi S. Palladium nanoparticles supported on modified crosslinked polyacrylamide containing phosphinite ligand: A novel and efficient heterogeneous catalyst for carbon–carbon cross-coupling reactions. Journal of Molecular Catalysis A: Chemical. 2010;322(1-2):98-105.

[12] Tamami B, Ghasemi S. Modified crosslinked polyacrylamide anchored Schiff base–cobalt complex: A novel nano-sized heterogeneous catalyst for selective oxidation of olefins and alkyl halides with hydrogen peroxide in aqueous media. Applied Catalysis A: General. 2011;393(1-2):242-50.

[13] Rashidi M, Blokhus AM, Skauge A. Viscosity and retention of sulfonated polyacrylamide polymers at high temperature. Journal of Applied Polymer Science. 2010;119(6):3623-9.

[14] Aalaie J, Vasheghani-Farahani E, Rahmatpour A, Semsarzadeh MA. Effect of montmorillonite on gelation and swelling behavior of sulfonated polyacrylamide nanocomposite hydrogels in electrolyte solutions. European Polymer Journal. 2008;44(7):2024-31.

[15] Kim K, Ju H, Kim J. Surface modification of BN/Fe3O4 hybrid particle to enhance interfacial affinity for high thermal conductive material. Polymer. 2016;91:74-80.

[16] Low LE, Tey BT, Ong BH, Tang SY. Unravelling pH-responsive behaviour of Fe3O4 @CNCs-stabilized Pickering emulsions under the influence of magnetic field. Polymer. 2018;141:93-101.

[17] Hanifehpour Y, Woo Joo S. Synthesis, characterization and sonophotocatalytic degradation of an azo dye on Europium doped cadmium selenide nanoparticles. Nanochemistry Research. 2018; 3(2): 178-88.

[18] Hosseinzadeh Z, Piryaei M, Babashpour Asl M, Abolghasemi MM. ZnO polythiophene SBA-15 nanoparticles as a solid-phase microextraction fiber for fast determination essential oils of Matricaria chamomilla. Nanochemistry Research. 2018; 3(2): 124-30.